Parametrization of the ^{2}H(γ, p)n reaction between 185 and 420 MeV

C. Steven Whisnant*
Physics Department, James Madison University, Harrisonburg, Virginia, 22807, USA
(Received 7 November 2005; published 12 April 2006)

A simple parametrization of the ^{2}H(γ, p)n cross-section data from LEGS, Mainz, and Bonn at laboratory photon energies between 187.5 and 420 MeV and the LEGS and Mainz beam asymmetry data between 185 and 412 MeV has been done. The fit represents both the energy and angular dependence of the cross section and asymmetry in terms of Legendre polynomials. A reduced χ^2 of 1.641 is obtained for the cross-section data with a total of 20 parameters. Three of the parameters are renormalization factors introduced to permit the three cross-section data sets to float relative to one another. The resulting renormalization factors are found to be well within the quoted systematic uncertainties for each experiment. The energy dependence of the parameters is in good agreement with fits done to the Mainz data at individual energies. The asymmetries are fit with an additional eight parameters with a reduced χ^2 of 1.229.

DOI: 10.1103/PhysRevC.73.044005 PACS number(s): 25.20.−x, 29.85.+c

I. INTRODUCTION

There now exist several high-quality data sets for the photodistintegration of the deuteron in the region of the Δ resonance. A global parametrization of those data is of practical interest for several reasons. First, in the absence of a free neutron target, the deuteron is a common choice of a nearly free neutron. An ingredient in the analysis of these experiments is knowledge of the photodisintegration cross sections and asymmetries. Second, in experiments using polarized targets that contain deuterium, the ability to normalize cross sections to this now well-known reaction is often important.

For the first purpose, a fast, simple functional form is desired since this is frequently required in a Monte Carlo simulation of an experiment. For the second purpose, a full propagation of experimental errors is required to include them in the systematics of the experiment being normalized. This work reports a fit to the data that satisfies both goals.

The cross-section data included in this analysis are the angular distributions obtained at LEGS [1], Mainz [2], and Bonn [3] between 187.5 and 420 MeV. These data sets, all obtained using monochromatic, tagged photon beams, were selected for their consistency, small experimental uncertainties, and energy coverage. The asymmetries are from LEGS [1] and Mainz [4]. These are the only data sets obtained with monochromatic beams with such a large coverage in both angle and energy.

Although Legendre polynomial fits to these cross sections were done by the experimenters, these are fits done at individual energies, primarily for the purpose of extracting the integrated cross section. As a result, the energy dependence of the coefficients is noisy, fluctuating with the scatter in the data from energy to energy. By imposing a smooth energy dependence, the trends with energy are more apparent and the uncertainties are smaller. The sole published parametrization of the asymmetries includes only the LEGS data and is a much more complicated multipole analysis [5]. There exists no simple form suitable for use in a Monte Carlo simulation.

Global fits to the cross sections using Legendre polynomials in the Δ-resonance region have been made previously. Thorlacius and Fearing [6] produced a fit to data spanning the range from 10 to 625 MeV. In this fit the statistical and systematic uncertainties were added in quadrature and each data set was fit separately to obtain the Legendre polynomial coefficients. These coefficients were then used as the "data" in the final fits. The energy dependence used in the global fit was a phenomenological form suggested by the presence of the Δ resonance.

The work of Rossi *et al*. [7] takes a different approach. Here, the total cross section is first fit to the monochromatic data then available and then the remaining data are *normalized to this fit* and only used to determine the shape of the angular distribution. For the fits to determine the total cross sections, the statistical and systematic uncertainties were added linearly.

There are several significant improvements that can be made to these earlier works. First, there have been additional high-quality monochromatic data obtained since these analyses were made. Of necessity, both analyses included many data sets obtained with untagged beams with more uncertain normalizations and larger scatter among the data sets. Second, neither work properly included the systematic uncertainties. Combining the statistical and systematic uncertainties as was done in these earlier efforts ignores the fundamental characteristic of the systematic uncertainties. The systematic uncertainties represent a common scale uncertainty that permits entire data sets to shift relative to another one without altering the shape of the distributions. By treating this uncertainty as if it were part of the angle- and energy-dependent statistical uncertainties, this commonality is not properly included. Finally, neither work reports the full covariance matrix. This makes it impossible to compute the uncertainty in the fitted function or to correctly assess the errors in a particular Legendre coefficient at a given energy. All of these issues are addressed in the present analysis.

*Electronic address: whisnacs@jmu.edu

The asymmetry data included in the fits are those of LEGS [1] and Mainz [4], spanning the energy range from 185 to 412 MeV. Largely because of the lack of quality data over a broad range of energies, no previous attempts to parametrize the beam asymmetries has been made. Reported here is the first such fit.

II. SPECIFICATION OF THE FIT

A. The fitting functions

The parametrization of the data requires the product of an energy-dependent and angle-dependent function. The angular dependence is most naturally represented by the Legendre polynomials, $P_l[\cos(\theta)]$, for the cross sections or associated Legendre polynomials, $P_l^2[\cos(\theta)]$, for the asymmetries [8]. After several trials using various orthogonal polynomials to represent the energy dependence, it was found to also be well reproduced by the Legendre polynomials. Since these functions are defined on the interval $[-1,1]$, the photon energies are scaled to fit this interval. The scaling is done by computing the average, $E_{\text{ave}} = \frac{1}{2}(E_{\max} + E_{\min})$, and half-width, $E_{\text{diff}} = \frac{1}{2}(E_{\max} - E_{\min})$, of the energy interval. The energies are mapped to the desired interval with the function

$$x(E) = \frac{E - E_{\text{ave}}}{E_{\text{diff}}}. \tag{1}$$

For all fits reported here, $E_{\max} = 430\,\text{MeV}$ and $E_{\min} = 180\,\text{MeV}$. With these definitions, the fitting function for the cross section can then be written as

$$\frac{d\sigma}{d\Omega}(\theta, E) = \sum_{k=0}^{6}\sum_{j=0}^{5} C_{jk} P_j[x(E)] P_k[\cos(\theta)], \tag{2}$$

where the C_{jk} are the parameters to be fit. For the asymmetry, the fit is done by parametrizing the numerator (the difference between cross sections obtained with parallel and perpendicular polarizations) and using the fitted cross section for the denominator,

$$\Sigma(\theta, E) = \frac{1}{\frac{d\sigma}{d\Omega}(\theta, E)} \sum_{k=2}^{6}\sum_{j=0}^{5} D_{jk} P_j[x(E)] P_k^2[\cos(\theta)]. \tag{3}$$

B. The cross-section fit procedure

The fit is done using the MINUIT function minimization package [9] to minimize χ^2. To fit the three cross-section data sets, each with an independent systematic error, the definition of χ^2 used here is described by D'Agostini [10] and is given by

$$\chi^2 = \sum_{n=1}^{3}\left[\sum_{i_n}\sum_{l_n}\left(\frac{\lambda_n\left(\frac{d\sigma}{d\Omega}\right)_{i_n l_n} - \frac{d\sigma}{d\Omega}\left(\theta_{i_n}, E_{l_n}\right)}{\lambda_n \sigma_{i_n l_n}}\right)^2 + \left(\frac{1-\lambda_n}{\delta_n}\right)^2\right], \tag{4}$$

where i_n and l_n label the angles and energies, respectively, and δ_n is the normalization uncertainty for the nth data set. By including a normalization factor, λ_n, for each data set, the sets are allowed to float relative to one another. Adding these three parameters to the 42 parameters (7 orders in angle $\times$ 6 orders in energy) in Eq. (2) gives a total of 45 parameters in the model.

Initially, a fit was made in which all parameters were allowed to vary starting with initial values of zero for all the C_{jk} and one for each of the λ_n. This produced a fit with 321 degrees of freedom (366 data points $-$ 45 parameters) and a reduced χ^2 of $\chi_\nu^2 = 1.560$.

The parameters were then checked for statistical significance using the F test [5,11]. Starting with the highest order coefficient, C_{76}, and proceeding in descending order, each coefficient was temporarily removed and the fit was redone, giving χ^2 values for fits both with, $\chi^2(m+1)$, and without, $\chi^2(m)$, each parameter. The F statistic with one degree of freedom is then given by

$$F_\chi = \frac{\chi^2(m) - \chi^2(m+1)}{\chi^2(m+1)/(N-m-1)} = \frac{\Delta\chi^2}{\chi_\nu^2}. \tag{5}$$

This quantity is compared with the critical value of $F_{\text{crit}} \approx 6.63$ [11] corresponding to a probability of 99% that the parameter in question is required to fit the data.

The normalization parameters were not included in this pruning process. The result of the procedure was that 20 parameters, 17 to parameterize the cross section and 3 normalizations, remain out of the 45.

C. The asymmetry fit procedure

Once the cross-section fit was complete, the parametrization of the cross section was fixed and the fit was made to the asymmetry using Eq. (3). The uncertainties reported for the LEGS asymmetries are the combined statistical and polarization-dependent systematic uncertainties. These two quantities are reported individually for the Mainz data set. For these fits, they are combined in quadrature as was done for the LEGS data set. Thus, there are no overall systematic errors to include in the asymmetry fits. The asymmetries for the two data sets are then fit with a χ^2 defined to be

$$\chi^2 = \sum_{n=1}^{2}\left[\sum_{i_n}\sum_{l_n}\left(\frac{\Sigma_{i_n l_n} - \Sigma\left(\theta_{i_n}, E_{l_n}\right)}{\sigma_{i_n l_n}}\right)^2\right]. \tag{6}$$

Since the cross section is held fixed at the best-fit value, there are 30 parameters (5 orders in angle $\times$ 6 orders in energy) in this fit. By fixing the cross section, the uncertainties in the asymmetry data are reflected in the resultant uncertainties of these additional parameters.

As was done for the cross section fits, the initial fit allowed all 30 parameters to vary starting from zero. This produced a fit with 198 degrees of freedom (228 data points $-$ 30 parameters) and $\chi_\nu^2 = 1.141$. Using the F test to prune the parameter space as was done before yields a final fit with 8 parameters.

TABLE I. The parameters obtained in the cross-section fit described in Sec. II B. The first three columns give the parameter number and the orders of the energy and angle polynomials, respectively. The fourth and fifth columns list the values from the fit and the square root of the diagonal element of the covariance matrix.

Parameter number	Energy order	Angle order	Value (μb/sr)	Uncertainty (μb/sr)
1	0	0	3.756	0.087
2	1	0	−1.988	0.047
3	2	0	−1.434	0.036
4	3	0	0.6506	0.024
5	4	0	0.3693	0.022
6	5	0	−0.1997	0.025
7	0	1	0.6798	0.019
8	1	1	−0.3175	0.018
9	2	1	−0.1546	0.025
10	3	1	0.1118	0.030
13	0	2	−0.8528	0.024
14	1	2	0.4790	0.025
26	1	4	0.3473	0.032
27	2	4	−0.2661	0.046
31	0	5	0.1218	0.022
37	0	6	−0.1574	0.025
39	2	6	0.2075	0.058

III. RESULTS

The fits to the cross sections and asymmetries are available on-line at http://acadine.physics.jmu.edu/~whisnacs/d2_param/. This Web site will generate the fitted values and the uncertainties in the fits for any angle and at any energy in the range of the fit. The parameters obtained and the computation of the reported uncertainties are described in detail in the following sections.

A. Cross-section parameters and uncertainties

The cross section parametrization obtained is given in Table I. The normalizations found from the fits were well within the reported scale uncertainties. As defined in Eq. (4), the difference between one and the fitted normalization factor, $(1 - \lambda)$, for each data set is to be compared with the systematic uncertainty assigned in each experiment. The normalization factors obtained are given in Table II.

TABLE II. The normalization parameters obtained in the fit described in Sec. II B. The first column indicates the data set. The second column cites the systematic uncertainty quoted by the experimenters. The third column gives the fitted normalization parameters. The fourth column gives the square root of the diagonal elements of the covariance matrix.

Data set	δ (%)	λ	σ_λ
LEGS	5.0	1.0197	0.024
Mainz	3.5	0.98063	0.023
Bonn	4.0	1.0118	0.023

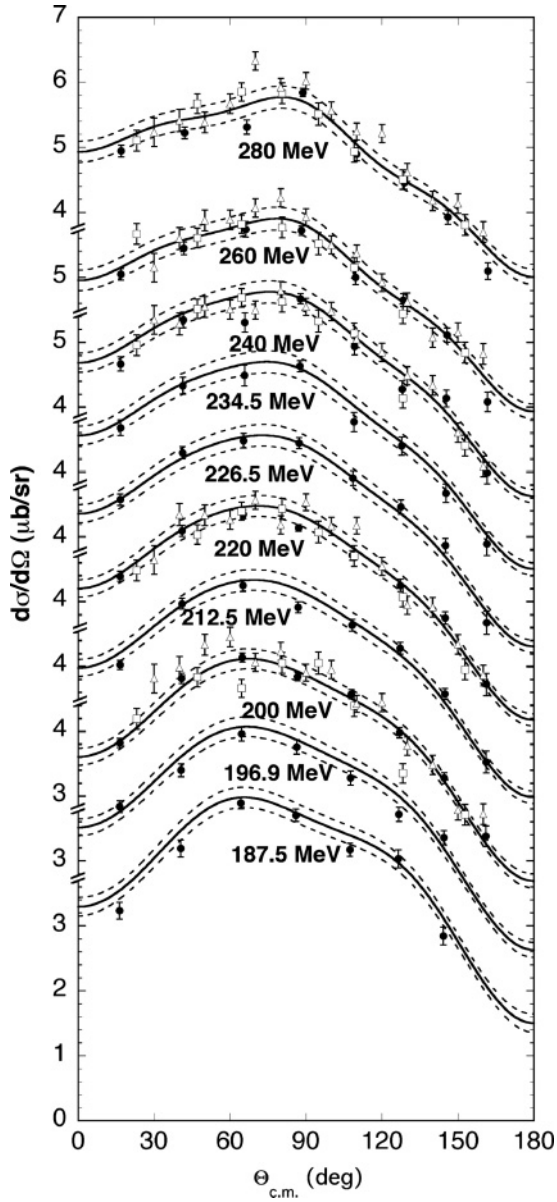

FIG. 1. Comparison of the LEGS, Mainz, and Bonn cross-section data with the fit. The LEGS data set is indicated with the filled circles, the Mainz data set is shown with open triangles, and the Bonn data set is indicated with open squares. The LEGS data set is plotted with the data from Mainz when within ≈4 MeV. The dashed lines represent $\pm\sqrt{s^2_{\rm fit}}$, the unbiased estimate of the uncertainty.

The total χ^2 for this fit is 567.75. With 346 degrees of freedom (366 data points and 20 parameters), this gives $\chi^2_\nu = 1.641$.

To use this fit to normalize experimental data, the full covariance matrix is required to compute the uncertainty in the computed cross section. The inclusion of the normalization factors in the fit includes the systematic uncertainties in the covariance matrix for the 17 functional parameters. Thus, the normalizations are implicitly included in the uncertainty computation using the 17×17 covariance matrix.

TABLE III. The covariance matrix obtained in the fit to the cross sections. The parameters are labeled by the parameter numbers listed in Table I.

	1	2	3	4	5	6	7	8	9	10
1	7.53×10^{-3}									
2	-3.98×10^{-3}	2.25×10^{-3}								
3	-2.86×10^{-3}	1.46×10^{-3}	1.33×10^{-3}							
4	1.28×10^{-3}	-6.62×10^{-4}	-5.54×10^{-4}	5.58×10^{-4}						
5	7.76×10^{-4}	-4.52×10^{-4}	-2.32×10^{-4}	4.06×10^{-5}	5.00×10^{-4}					
6	-4.15×10^{-4}	3.32×10^{-4}	4.74×10^{-5}	1.34×10^{-5}	-9.17×10^{-5}	6.11×10^{-4}				
7	1.35×10^{-3}	-7.19×10^{-4}	-5.06×10^{-4}	2.43×10^{-4}	1.23×10^{-4}	-9.54×10^{-5}	3.53×10^{-4}			
8	-6.32×10^{-4}	3.40×10^{-4}	2.60×10^{-4}	-1.12×10^{-4}	-6.68×10^{-5}	1.41×10^{-5}	-1.11×10^{-4}	3.33×10^{-4}		
9	-2.95×10^{-4}	1.84×10^{-4}	8.38×10^{-5}	-4.42×10^{-5}	-2.85×10^{-5}	5.62×10^{-5}	-8.20×10^{-5}	-1.63×10^{-5}	6.26×10^{-4}	
10	2.35×10^{-4}	-1.20×10^{-4}	-7.25×10^{-5}	1.03×10^{-5}	7.69×10^{-5}	2.05×10^{-5}	5.87×10^{-6}	2.64×10^{-5}	-1.25×10^{-4}	9.07×10^{-4}
13	-1.70×10^{-3}	9.07×10^{-4}	6.60×10^{-4}	-2.89×10^{-4}	-1.69×10^{-4}	7.09×10^{-5}	-3.23×10^{-4}	1.63×10^{-4}	9.32×10^{-5}	-2.82×10^{-5}
14	9.66×10^{-4}	-5.01×10^{-4}	-3.42×10^{-4}	1.85×10^{-4}	7.97×10^{-5}	-5.63×10^{-5}	1.91×10^{-4}	-8.41×10^{-5}	2.13×10^{-5}	4.29×10^{-5}
26	7.05×10^{-4}	-3.37×10^{-4}	-2.47×10^{-4}	1.38×10^{-4}	3.60×10^{-5}	-3.62×10^{-5}	1.54×10^{-4}	-1.05×10^{-4}	4.38×10^{-5}	-4.38×10^{-6}
27	-5.21×10^{-4}	3.14×10^{-4}	2.29×10^{-4}	-5.26×10^{-5}	-2.12×10^{-5}	-1.62×10^{-5}	-1.16×10^{-4}	1.34×10^{-4}	-1.29×10^{-4}	1.33×10^{-4}
31	2.38×10^{-4}	-1.19×10^{-4}	-1.01×10^{-4}	4.23×10^{-5}	2.22×10^{-5}	-4.85×10^{-6}	7.86×10^{-5}	4.96×10^{-6}	-7.39×10^{-7}	-1.90×10^{-5}
37	-2.86×10^{-4}	1.82×10^{-4}	8.44×10^{-5}	-5.47×10^{-5}	-1.97×10^{-5}	4.62×10^{-5}	-6.99×10^{-5}	5.32×10^{-5}	-6.14×10^{-6}	-5.38×10^{-5}
39	3.80×10^{-4}	-2.23×10^{-4}	-2.04×10^{-5}	1.29×10^{-4}	-2.52×10^{-5}	-1.01×10^{-4}	3.05×10^{-5}	-1.23×10^{-5}	-1.71×10^{-4}	2.17×10^{-4}
λ_{LEGS}	2.04×10^{-3}	-1.09×10^{-3}	-7.71×10^{-4}	3.56×10^{-4}	2.05×10^{-4}	-1.15×10^{-4}	3.69×10^{-4}	-1.76×10^{-4}	-8.16×10^{-5}	6.28×10^{-5}
λ_{Mainz}	1.95×10^{-3}	-1.03×10^{-3}	-7.44×10^{-4}	3.34×10^{-4}	1.89×10^{-4}	-1.01×10^{-4}	3.52×10^{-4}	-1.63×10^{-4}	-8.21×10^{-5}	5.51×10^{-5}
λ_{Bonn}	2.02×10^{-3}	-1.06×10^{-3}	-7.74×10^{-4}	3.52×10^{-4}	1.99×10^{-4}	-1.06×10^{-4}	3.65×10^{-4}	-1.70×10^{-4}	-8.18×10^{-5}	6.29×10^{-5}

Using the standard uncertainty propagation equation [11], we can compute the uncertainty in the fitted function, δf, from

$$(\delta f)^2 = \sum_r \sum_s \left(\frac{\partial f}{\partial C_r}\right) \sigma_{rs}^2 \left(\frac{\partial f}{\partial C_s}\right), \tag{7}$$

where the indices r and s run over parameter numbers as listed in column 1 of Table I and σ_{rs}^2 is the corresponding covariance. The derivatives are given by

$$\frac{\partial f}{\partial C_i} = P_{j_i}[x(E)] P_{k_i}[\cos(\theta)], \tag{8}$$

where i is the parameter number and j_i and k_i are the corresponding energy and angle polynomial orders, repectively, taken from Table I. Using integer arithmetic (truncation to an integer after division), j_i and k_i are related to the parameter number i by $k_i = \frac{1}{6}(i-1)$ and $j_i = (i-1) - 6k_i$.

The covariances obtained from the fit are given in Tables III and IV. With these covariances and Eqs. (7) and (8), the standard deviation of the fit can be calculated at any point.

A model dependence in the fit or non-Gaussian distribution of the experimental uncertainties leads to $\chi_\nu^2 > 1$. When this occurs, the uncertainty on the fit derived solely from the covariance matrix does not have the expected meaning that for approximately 68% of the data $|\text{fit} - \text{data}| \leqslant$ uncertainty on the fit. The appropriate uncertainty to use to retain this interpretation is the *unbiased estimator* [12,13]. The unbiased estimate of the covariances, s_{rs}^2, is related to the covariances given in Tables III and IV, σ_{rs}^2, by the reduced χ^2 for the fit, $s_{rs}^2 = \chi_\nu^2 \sigma_{rs}^2$. Since Eq. (7) is linear with respect to σ_{rs}^2, this same relation holds for the unbiased estimator of the uncertainty in the fitted function

$$s_{\text{fit}}^2 = \chi_\nu^2 (\delta f)^2 . \tag{9}$$

It is this unbiased estimate that is quoted here. Note that, although covariances returned by MINUIT must be multiplied by χ_ν^2, other software packages handle this issue differently. For example, those returned by the E04FDF routine in the NAG library [14] are unbiased estimates and so do not need this extra factor inserted.

A well-known example of an unbiased estimator of the uncertainty in a data set is the usual variance or its square root, the standard deviation of the data about the mean. This quantity has the property that approximately 68% of the data points lie within ± 1 standard deviation of the mean. This same property is also true for the unbiased estimator used here and will be examined in Sec. III C.

B. Asymmetry parameters and uncertainties

The asymmetry parametrization is given in Table V. The total χ^2 for this fit is 270.44. With 220 degrees of freedom (228

TABLE IV. The covariance matrix for the cross-section fit continued from Table III.

	13	14	26	27	31	37	39	λ_{LEGS}	λ_{Mainz}	λ_{Bonn}
13	5.65×10^{-4}									
14	-1.76×10^{-4}	6.23×10^{-4}								
26	-9.21×10^{-5}	1.96×10^{-4}	1.05×10^{-3}							
27	1.54×10^{-4}	6.83×10^{-5}	-8.91×10^{-5}	2.08×10^{-3}						
31	-8.37×10^{-5}	8.78×10^{-5}	1.18×10^{-4}	-2.44×10^{-5}	5.01×10^{-4}					
37	1.23×10^{-4}	4.03×10^{-5}	8.45×10^{-5}	3.09×10^{-5}	-5.46×10^{-5}	6.26×10^{-4}				
39	-6.56×10^{-5}	1.43×10^{-4}	2.36×10^{-4}	5.34×10^{-4}	6.31×10^{-5}	-2.45×10^{-4}	3.39×10^{-3}			
λ_{LEGS}	-4.62×10^{-4}	2.60×10^{-4}	1.83×10^{-4}	-1.51×10^{-4}	6.94×10^{-5}	-8.79×10^{-5}	1.15×10^{-4}	5.58×10^{-4}		
λ_{Mainz}	-4.43×10^{-4}	2.49×10^{-4}	1.82×10^{-4}	-1.34×10^{-4}	6.20×10^{-5}	-8.37×10^{-5}	1.14×10^{-4}	5.28×10^{-4}	5.15×10^{-4}	
λ_{Bonn}	-4.57×10^{-4}	2.57×10^{-4}	1.89×10^{-4}	-1.42×10^{-4}	6.52×10^{-5}	-7.98×10^{-5}	1.03×10^{-4}	5.46×10^{-4}	5.22×10^{-4}	5.48×10^{-4}

TABLE V. The parameters obtained in the asymmetry fit described in Sec. II C. The first three columns give the parameter number and the orders of the energy and angle polynomials, respectively. The third column lists the values from the fit. The right-most column lists the square root of the diagonal elements of the covariance matrix listed in Table VI.

Parameter number	Energy order	Angle order	Value	Uncertainty
1	0	2	−0.3972	0.0041
2	1	2	0.1629	0.0052
3	2	2	0.2015	0.0083
4	3	2	−0.1207	0.010
7	0	3	0.02670	0.0020
9	2	3	0.01018	0.0046
13	0	4	0.01406	0.0014
14	1	4	0.01089	0.0024

data points and 8 parameters), $\chi^2_\nu = 1.229$. The full covariance matrix is listed in Table VI.

Since the cross section is fixed at the best-fit parametrization described above, the uncertainty in the asymmetry is also given by Eq. (7) (now taking dervatives with respect to the D_i), where the indices r and s run over parameter numbers as listed in column 1 of Table V and σ^2_{rs} is the corresponding covariance. The necessary derivatives are given by

$$\frac{\partial f}{\partial D_i} = P_{j_i}[x(E)]P^2_{k_i}[\cos(\theta)], \tag{10}$$

where i is the parameter number and j_i and k_i are the corresponding energy and angle polynomial orders, repectively, taken from Table V. Using integer arithmetic, j_i and k_i are related to the parameter number i by $k_i = \frac{1}{6}(i-1)+2$ and $j_i = (i-1) - 6(k_i - 2)$.

C. Comparison with the data

The 366 cross-section data points included in the fit comprise 37 angular distributions ranging from 187.5 to 420 MeV in laboratory photon energy. To present the results of the fit, the data have been grouped into 19 energy bins. The Mainz and Bonn energies match throughout the energy range. When the LEGS data are within ≈4 MeV, they are plotted with the other two sets.

The comparison of the fits and the data is shown in Figs. 1 and 2. The unbiased estimate of the uncertainty in the fit, $\pm\sqrt{s^s_{\rm fit}}$, is indicated by the dashed lines above and below each fit. The data plotted here are the unrenormalized data as reported by the authors. Since the renormalization factors are only a few percent different from unity, it is difficult to see the small shifts that their inclusion would make on the plot.

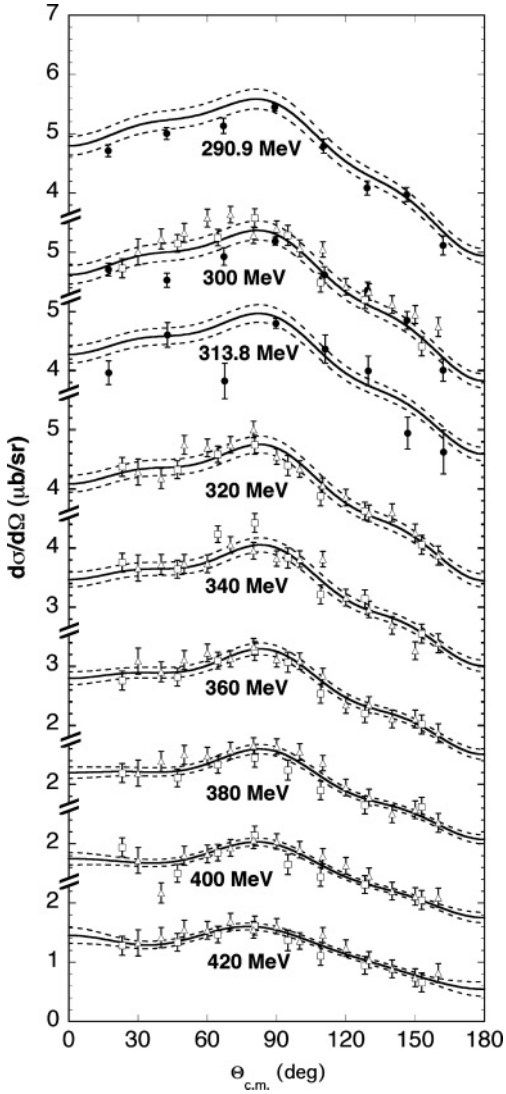

FIG. 2. Comparison of the LEGS, Mainz, and Bonn cross-section data with the fit at energies between 290.0 and 420 MeV. Symbols have the same meaning as in Fig. 2.

TABLE VI. The covariance matrix obtained in the asymmetry fit. The parameters are labeled by the parameter numbers listed in Table V.

	1	2	3	4	7	9	13	14
1	1.66×10^{-5}							
2	1.01×10^{-5}	2.73×10^{-5}						
3	-4.38×10^{-6}	3.06×10^{-6}	6.81×10^{-5}					
4	-1.23×10^{-5}	-2.46×10^{-5}	1.01×10^{-5}	1.01×10^{-4}				
7	1.62×10^{-6}	4.12×10^{-6}	3.82×10^{-7}	2.83×10^{-6}	3.82×10^{-6}			
9	-5.42×10^{-6}	-1.24×10^{-5}	-6.44×10^{-6}	-9.60×10^{-6}	-1.95×10^{-6}	2.11×10^{-5}		
13	-3.04×10^{-7}	-7.04×10^{-7}	6.98×10^{-7}	2.05×10^{-6}	3.30×10^{-7}	-9.10×10^{-7}	1.84×10^{-6}	
14	-1.44×10^{-6}	-1.78×10^{-6}	2.00×10^{-6}	4.03×10^{-6}	7.39×10^{-8}	-8.06×10^{-7}	1.97×10^{-6}	5.76×10^{-6}

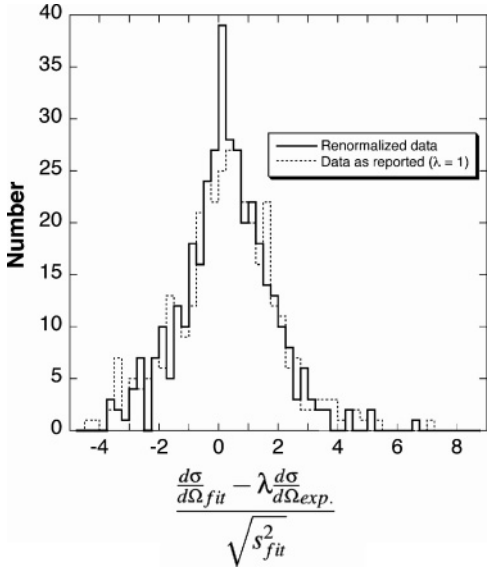

FIG. 3. A histogram of the difference between the cross-section fit and the data divided by the unbiased uncertainty in the fit. The solid line represents the difference computed with the data rescaled by the normalization factors obtain in the fit (Table II). The dashed line shows the difference computed with the data as reported.

To make the changes produced by the renormalization more apparent, a histogram of the difference between the fit and the data divided by the uncertainty in the fit is shown in Fig. 3.

In this figure, the solid line represents the difference computed with the data rescaled by the normalizations given in Table II. Integrating the histogram symmetrically about the mean shows that 57% of the rescaled data lie within $\pm\sqrt{s^2_{\rm fit}}$ of the fit. The dashed line represents the same quantity using the data as reported. The same integral for this data gives 52% of the data within the fitted error band. From the definition of $s^2_{\rm fit}$, 68% of the rescaled data are expected in this interval.

This histogram also makes clear that the distribution of the data is not symmetric and shows that there are more outliers than are expected from a Gaussian distribution. Nevertheless, $\sqrt{s^2_{\rm fit}}$ gives a reasonable estimate of the uncertainty in the fit. The character of the distribution of differences suggests that in addition to the angle- and energy-independent experimental systematic uncertainties, there are perhaps also energy- and perhaps even angle-dependent systematic effects that are impossible to estimate. Introducing an overall scale factor for the uncertainties to find the interval that contains ≈68% inherently assumes that the systematic scale uncertainties are too small and this is clearly not the case.

The 228 asymmetry data points comprise 31 angular distributions, spanning the energy range from 185 to 412 MeV. As was done for the cross sections, when the LEGS data are within ≈4 MeV of the Mainz energy, the two data sets are plotted together. The resulting 20 energy bins are shown in Figs. 4 and 5.

The quality of the fit is again most easily displayed in a histogram of the difference between the data and the fitted asymmetry divided by the uncertainty on the fit. This is shown in Fig. 6. The solid line represents the histogram of all the

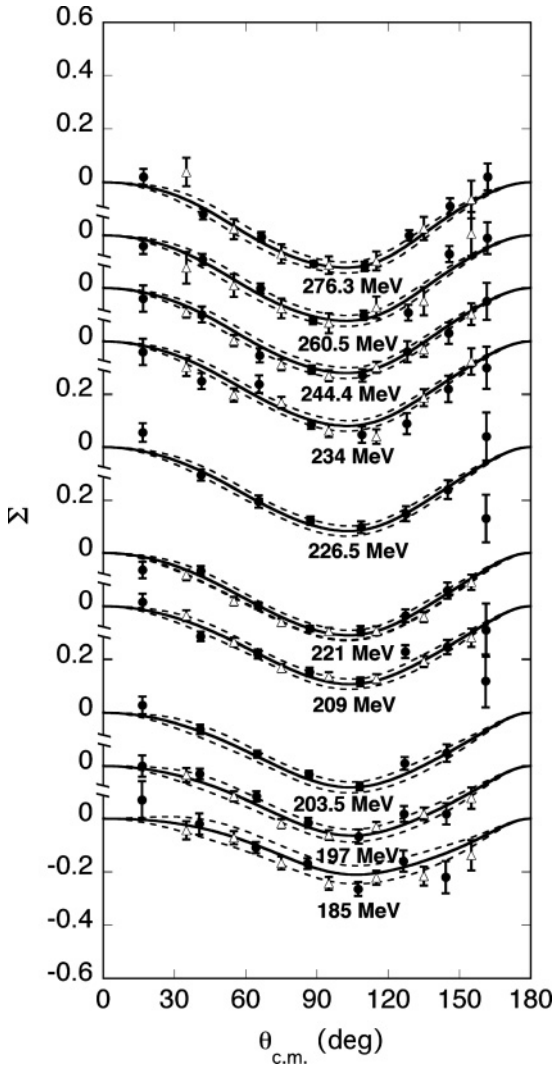

FIG. 4. Comparison of the LEGS and Mainz asymmetries between 185 and 276 MeV with the fit. The LEGS data are indicated with the filled circles; the Mainz data are shown with open triangles.

data included in the fit. Unlike the cross-section histogram, there is a significant tail extending to values much larger than $\pm\sqrt{s^2_{\rm fit}}$. This happens because the fitting function and its uncertainties are required to vanish at 0° and 180°. This constraint forces the uncertainty in the fit to be smaller than a simple inspection of the scatter in the data at these angles would suggest. The fraction of the total 228 data points that lie within $\pm\sqrt{s^2_{\rm fit}}$ is 0.34, much smaller than expected. To see the effect of relaxing this constraint, a histogram using only data for which $85^\circ \geqslant \theta_{\rm c.m.} \geqslant 115^\circ$ is shown with the dashed line. For the data near 90°, the influence of the constraint is minimal and the computed uncertainties do reflect the full spread of the data. Of the 61 data points in this angular range, the fraction within $\pm\sqrt{s^2_{\rm fit}}$ of the mean is 0.72, in good agreement with the expected 2/3. Thus, the large tails on this distribution do not indicate a failure of the model or an underestimate in the experimental uncertainties. Rather, they simply reflect the constraints imposed by the model used.

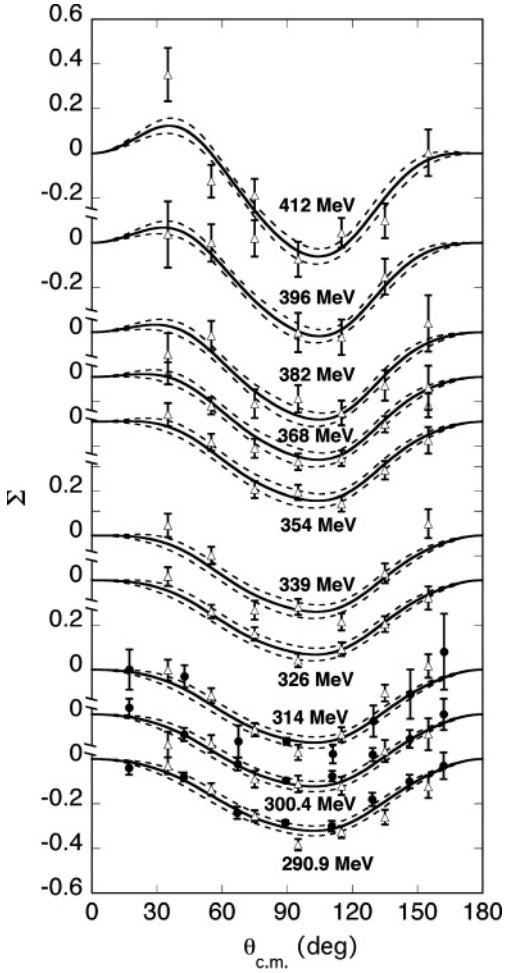

FIG. 5. Comparison of the LEGS and Mainz asymmetries between 290.9 and 412 MeV with the fit. The symbols have the same meaning as in Fig. 4.

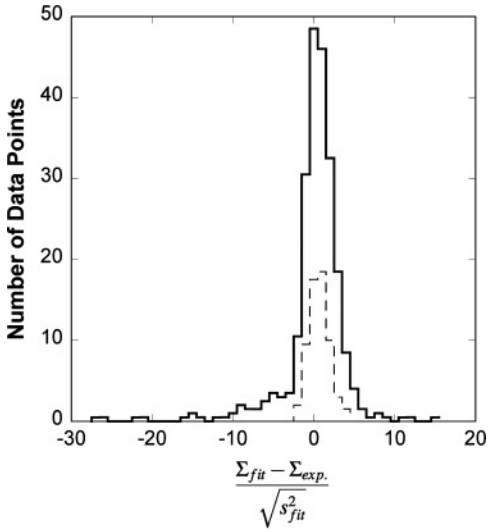

FIG. 6. A histogram of the difference between the asymmetry fit and the data divided by the unbiased uncertainty in the fit. The solid line represents the difference computed with all the data points. The dashed line shows the result when only data between 85° and 115° are included.

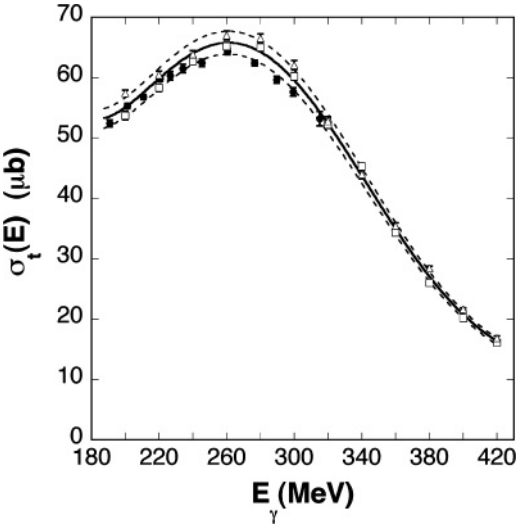

FIG. 7. The energy dependence of the angle-integrated cross section. The unbiased estimate of the uncertainties in the fit are shown with dashed lines above and below the fitted results. The symbols have the same meaning as in Fig. 1.

IV. DISCUSSION

Using the well-known properties of the Legendre polynomials, the angle-integrated cross sections are readily computed. Integrating Eq. (2) over all solid angle gives 4π times the coefficient of the $k = 0$ term in Eq. (2),

$$\sigma_t(E) = \int \frac{d\sigma}{d\Omega}(\theta, E)\, d\Omega = 4\pi \sum_{j=0}^{5} C_{j0} P_j[x(E)], \qquad (11)$$

and the propagated uncertainty is

$$[\delta\sigma_t(E)]^2 = (4\pi)^2 \sum_{r=0}^{5}\sum_{s=0}^{5} P_r[x(E)] s_{rs}^2 P_s[x(E)], \qquad (12)$$

where s_{rs}^2 is the unbiased estimator of the covariance between parameters C_{r0} and C_{s0}, $s_{rs}^2 = \sigma_{rs}^2 \chi_\nu^2$. A comparison of the total cross section from this fit with that obtained by fits made by the experimenters to the individual data sets is shown in Fig. 7.

Similarly, the energy-dependent coefficients for $k > 0$ can be written

$$A_k(E) = \sum_{j=0}^{5} C_{jk} P_j[x(E)] \qquad (13)$$

with an uncertainty of

$$[\delta A_k(E)]^2 = \sum_{r=0}^{5}\sum_{s=0}^{5} P_r[x(E)]\,(s_{rs})_k^2\, P_s[x(E)], \qquad (14)$$

where $(s_{rs})_k^2$ is the unbiased covariance between parameters C_{rk} and C_{sk}. The energy dependences of these coefficients are shown along with their uncertainties in Fig. 8. These curves are compared with the coefficients obtained by Mainz [2] and Bonn [3]. These coefficients are the result of fitting each

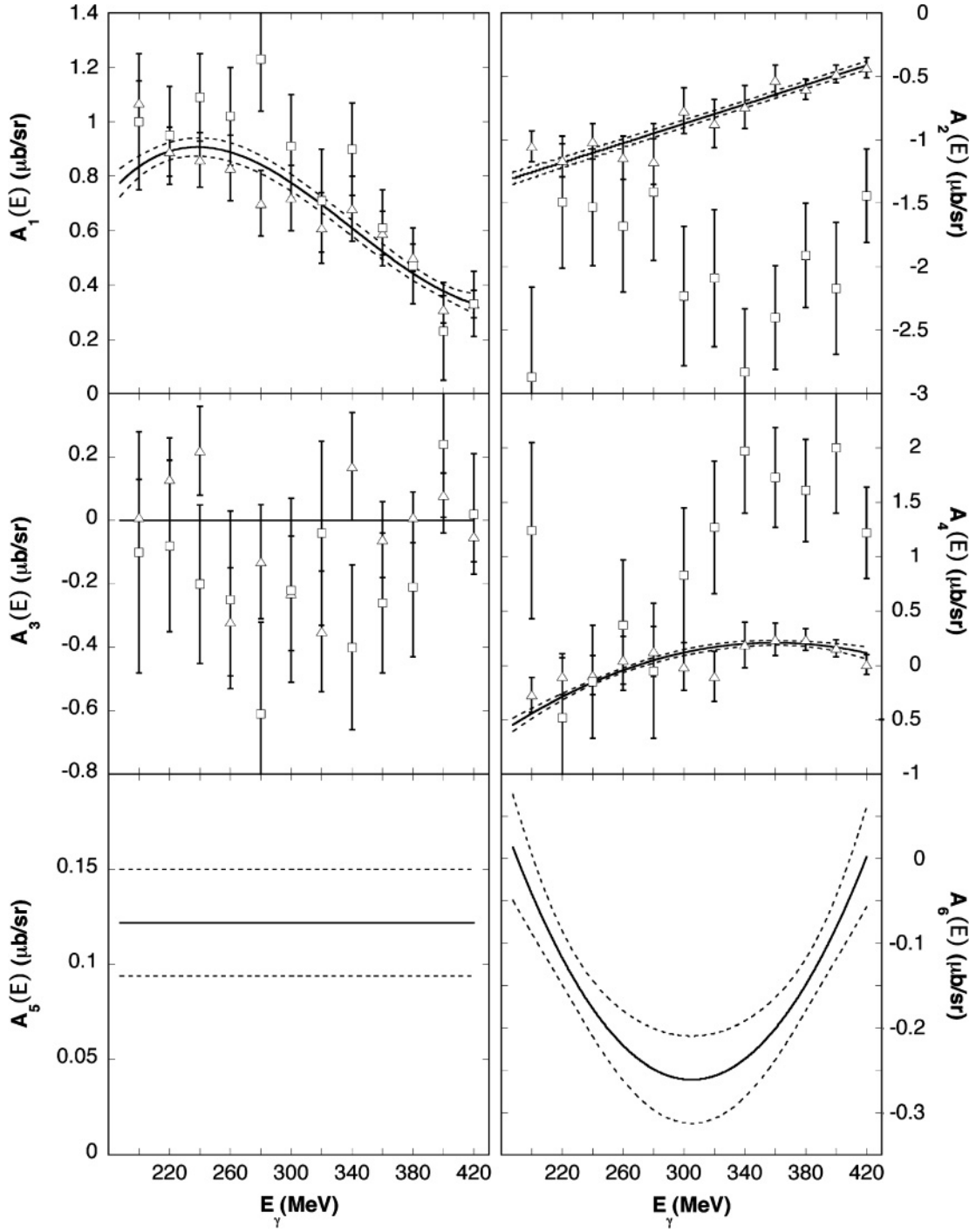

FIG. 8. The energy dependence of the $A_k(E)$ coefficients. Plotted as open triangles are the coefficients from Ref. [2]. The open squares represent coefficients obtained from the Bonn [3] data.

energy separately with a fourth-order polynomial; hence, no comparison can be made for A_5 and A_6.

As can be seen in Fig. 8, the present fit gives a good representation of the coefficients obtained in the individual fits to the Mainz data. Even for A_3, which is exactly zero here owing to its exclusion from the fit by the F-test pruning of the parameter space, we find reasonable agreement given the scatter in the individual fits. Somewhat surprising, however, is the appearance of the A_5 and A_6 terms, which have been omitted previously for all fits done at any energy in this range but were not excluded by the F-test pruning of the fit function described in Sec. II B. That these terms are required by the data in an energy-dependent fit suggests that the truncated fits are compensating by shifting the relatively small missing strength to lower order terms [15]. Such a shift of higher order strength has been found in multipole analyses using

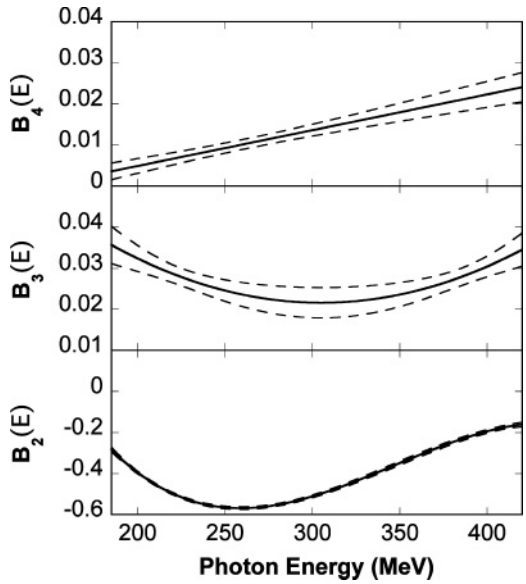

FIG. 9. The energy dependence of the cross-section difference, $\Sigma(\theta, E) \cdot \frac{d\sigma}{d\Omega}(\theta, E)$. The uncertainty in the parameters, $\pm\sqrt{s^2_{\rm fit}}$, is shown as dashed lines above and below the fitted results.

Legendre polynomials [12] so that even fits with orthogonal functions are not immune. Moreover, the uncertainties in the highest order coefficients are expected to be largest [16] as is seen here. When the small A_5 and A_6 coefficients with their relatively large uncertainties are removed and their strength is redistributed among the lower order coefficients, the changes are difficult to discern given the larger uncertainties of the Mainz fits. Perhaps the most noticeable occurrence of this shift is from $A_5 \rightarrow A_3$, where A_3 is exactly zero in the energy-dependent fit but appears to be more consistently negative in the Mainz fit, although even here the scatter in the parameters from energy to energy makes the effect difficult to quantify.

Although the Mainz coefficients have large uncertainties, they generally agree with the energy-dependent fits. However, the Bonn data have much larger uncertainties and show much larger differences from the current fits, particularly for the A_2 and A_4 coefficients. The variation of these coefficients appears to be correlated (i.e., when A_2 decreases, A_4 increases). It is possible that A_1 and A_3 also display a small correlation, but the uncertainties are too large to identify it with certainty. To ensure that this ambiguity is not a problem, more data must be included in the fit [12]. The Mainz coefficients are fit to 14 data points per energy compared to the 8 data points per energy in the Bonn data. The two data sets have comparable statistical uncertainties. Thus, the increase in the data included in the fit appears to be the source of the improvement in the Mainz coefficients compared to those obtained from the Bonn data. Because a much more complete data set is included in this analysis, the higher order coefficients are required here. Nevertheless, there is good agreement among all approaches for A_0, the angle-integrated cross section. The scatter is small and it is consistently determined by all analyses.

Because of the smooth energy dependence imposed and the inclusion of all the data in one fit, the uncertainties in the energy-dependent coefficients are generally much smaller than found previously. The one exception is the total cross section (Fig. 7), where the unbiased estimate of the uncertainty in the fit includes the statistical uncertainty in the data along with the scatter among the data sets. A comparison of the total cross sections determined by the present fit with those of the experimenters, as described in the discussion of the full data set in Sec. III C, shows that the data are distributed consistently with expectations. The difference between the data as reported and the fit is within $\pm\sqrt{s^s_{\rm fit}}$ 67% of the time (for 24 out of the 36 data points). Renormalizing the data with the factors given in Table II yields 72% of the data within $\pm\sqrt{s^s_{\rm fit}}$ of the fit (26 out of 36). Given the small number of data points and the modest renormalization factors, the effect of the renormalization is difficult to quantify with any precision. Nevertheless, it is clearly consistent with expectations.

The choice of parametrization of the asymmetry makes it impossible to generate an angle-independent set of coefficients. However, the cross-section difference, $\Sigma(\theta, E) \cdot \frac{d\sigma}{d\Omega}(\theta, E)$, can be separated this way to give

$$\Sigma(\theta, E) \cdot \frac{d\sigma}{d\Omega}(\theta, E) = \sum_{k=2}^{6} \left(\sum_{j=0}^{5} D_{jk} P_j[x(E)] \right) P_k^2[\cos(\theta)]. \tag{15}$$

The angle-independent energy coefficient is delimited by the parentheses and is given by

$$B_k = \sum_{j=0}^{5} D_{jk} P_j[x(E)]; \tag{16}$$

the uncertainty in the cross section difference is given by

$$[\delta B_k(E)]^2 = \sum_{r=0}^{5} \sum_{s=0}^{5} P_r[x(E)]\,(s_{rs})^2_k\,P_s[x(E)], \tag{17}$$

where the $(s_{rs})^2_k$ are the unbiased covariances computed from Table VI. These coefficients are shown in Fig. 9.

Note that the full experimental uncertainty in the asymmetry is given in these coefficients since the fitted cross sections are included as values with no uncertainty in the asymmetry fit. Although this is not the case for experimentally determined differences and asymmetries, the fitting method chosen here forces this to be the case. Since this sort of analysis of beam asymmetries has not been done before, there are no coefficients with which to compare.

V. SUMMARY

Presented here is an energy- and angle-dependent fit to the photodisintegration of deuterium in the energy range from 185 to 420 MeV. The results for the cross section are in good agreement with the results of earlier fits done at individual energies and the uncertainties are substantially smaller. The fit to the asymmetry gives a good representation of the data and, when combined with the cross-section fit, is a useful input to

Monte Carlo simulations. The simple parametrization of the modern data, obtained with monochromatic photon beams, makes it possible to use this as a benchmark for normalizing data from new experiments obtained with deuteron targets, especially with polarized targets.

ACKNOWLEDGMENTS

The author wishes to thank Dr. Andrew Sandorfi for the many productive conversations during the course of this work. This work is supported in part by the National Science Foundation.

[1] LEGS Collaboration, G. Blanpied *et al.*, Phys. Rev. C **61**, 024604 (1999).
[2] R. Crawford *et al.*, Nucl. Phys. **A603**, 303 (1996).
[3] J. Arends, H. J. Gassen, A. Hegerath, B. Mecking, G. Nöldeke, P. Prenzel, T. Reichelt, A. Voswinkel, and W. W. Sapp, Nucl. Phys. **A412**, 509 (1984).
[4] S. Wartenberg, J. Ahrens, J. Annand, H. J. Arends, G. Audit, R. Beck, A. Braghieri, N. d'Hose, S. Hall, E. Heid, V. Isbert, J. D. Kellie, H. P. Krahn, J. C. McGeorge, R. O. Owens, A. Panzeri, P. Pedroni, T. Pinelli, G. Tamas, and A. Thomas, Few-Body Syst. **26**, 213 (1999).
[5] C. S. Whisnant, W. K. Mize, D. Pomaréde, and A. M. Sandorfi, Phys. Rev. C **58**, 289 (1998).
[6] A. E. Thorlacius and H. W. Fearing, Phys. Rev. C **33**, 1830 (1986).
[7] P. Rossi, E. De Sanctis, P. Levi Sandri, N. Bianchi, C. Guaraldo, V. Lucherini, V. Muccifora, E. Polli, A. R. Reolon, and G. M. Urciuoli, Phys. Rev. C **40**, 2412 (1989).
[8] A. Cambi, B. Mosconi, and P. Ricci, Phys. Rev. C **26**, 2358 (1982).
[9] F. James and M. Roos, Comput. Phys. Commun. **10**, 343 (1975). Current version of the code is available at http://wwwasd.web.cern.ch/wwwasd/cernlib/download/2005_source/.
[10] G. D'Agostini, Nucl. Instrum. Methods Phys. Res. A **346**, 306 (1994).
[11] P. R. Bevington and D. K. Robinson, *Data Reduction and Error Analysis for the Physical Sciences*, 2nd ed. (McGraw-Hill, New York, 1992), p. 43.
[12] LEGS Collaboration, G. Blanpied *et al.*, Phys. Rev. C **64**, 025203 (2001).
[13] J. R. Wolberg, *Prediction Analysis* (Van Nostrand, New York, 1967), pp. 62–63.
[14] Numerical Algorithms Group, Ltd. Wilkinson House, Jordon Hill Road, Oxford OX2-8DR, UK.
[15] A. Donnachie, Rep. Prog. Phys. **36**, 695 (1973).
[16] J. E. Bowcock and H. Burkhardt, Rep. Prog. Phys. **38**, 1099 (1975).